

Distribution of donor states on the surface of AlGaN/GaN heterostructures

Yue-Bo Liu(柳月波), Hong-Hui Liu(刘红辉), Jun-Yu Shen(沈俊宇), Wan-Qing Yao(姚婉青), Feng-Ge Wang(王风格), Yuan Ren(任远), Min-Jie Zhang(张敏杰), Zhi-Sheng Wu(吴志盛), Yang Liu(刘扬), and Bai-Jun Zhang(张佰君)

Citation: Chin. Phys. B, 2021, 30 (**12**): 128102. DOI: 10.1088/1674-1056/ac0792
Journal homepage: http://cpb.iphy.ac.cn; http://iopscience.iop.org/cpb

What follows is a list of articles you may be interested in

Characteristics of AlGaN/GaN high electron mobility transistors on metallic substrate

Minglong Zhao(赵明龙), Xiansheng Tang(唐先胜), Wenxue Huo(霍雯雪), Lili Han(韩丽丽), Zhen Deng(邓震), Yang Jiang(江洋), Wenxin Wang(王文新), Hong Chen(陈弘), Chunhua Du(杜春花), Haiqiang Jia(贾海强)

Chin. Phys. B, 2020, 29 (**4**): 048104. DOI: 10.1088/1674-1056/ab7d9c

A new sulfur-doped source and synergistic effect with nitrogen for carbon dots produced from glucose

Lige Fu(付丽歌), Yuehong Yin(殷月红), Guohua Cao(曹国华), Pingping Wu(武苹苹), Jian Wang(汪舰), Lingling Yan(闫玲玲), Baoqing Zhang(张宝庆), Ming Li(李明)

Chin. Phys. B, 2019, 28 (**12**): 128102. DOI: 10.1088/1674-1056/ab5213

High-performance InAlGaN/GaN enhancement-mode MOS-HEMTs grown by pulsed metal organic chemical vapor deposition

Ya-Chao Zhang(张雅超), Zhi-Zhe Wang(王之哲), Rui Guo(郭蕊), Ge Liu(刘鸽), Wei-Min Bao(包为民), Jin-Cheng Zhang(张进成), Yue Hao(郝跃)

Chin. Phys. B, 2019, 28 (**1**): 018102. DOI: 10.1088/1674-1056/28/1/018102

Influence of adatom migration on wrinkling morphologies of AlGaN/GaN micro-pyramids grown by selective MOVPE

Jie Chen(陈杰), Pu-Man Huang(黄溥曼), Xiao-Biao Han(韩小标), Zheng-Zhou Pan(潘郑州), Chang-Ming Zhong(钟昌明), Jie-Zhi Liang(梁捷智), Zhi-Sheng Wu(吴志盛), Yang Liu(刘扬), Bai-Jun Zhang(张佰君)

Chin. Phys. B, 2017, 26 (**6**): 068101. DOI: 10.1088/1674-1056/26/6/068101

L_g=100 nm T-shaped gate AlGaN/GaN HEMTs on Si substrates with non-planar source/drain regrowth of highly-doped n^+-GaN layer by MOCVD

Huang Jie, Li Ming, Tang Chak-Wah, Lau Kei-May

Chin. Phys. B, 2014, 23 (**12**): 128102. DOI: 10.1088/1674-1056/23/12/128102

Distribution of donor states on the surface of AlGaN/GaN heterostructures*

Yue-Bo Liu(柳月波)[1], Hong-Hui Liu(刘红辉)[1], Jun-Yu Shen(沈俊宇)[1], Wan-Qing Yao(姚婉青)[1], Feng-Ge Wang(王风格)[1], Yuan Ren(任远)[1], Min-Jie Zhang(张敏杰)[1], Zhi-Sheng Wu(吴志盛)[1,2], Yang Liu(刘扬)[1,2], and Bai-Jun Zhang(张佰君)[1,2,†]

[1] *School of Electronics and Information Technology, Sun Yat-sen University, Guangzhou* 510006, *China*
[2] *State Key Laboratory of Optoelectronic Materials and Technologies, Sun Yat-sen University, Guangzhou* 510275, *China*

(Received 10 March 2021; revised manuscript received 3 June 2021; accepted manuscript online 3 June 2021)

The uniform distribution model of the surface donor states in AlGaN/GaN heterostructures has been widely used in the theoretical calculation. A common and a triple-channel AlGaN/GaN heterostructure Schottky barrier diodes have been fabricated to verify the models, but the calculation results show the uniform distribution model can not provide enough electrons to form three separate 2DEGs in the triple-channel AlGaN/GaN heterostructure. Our experiments indicate the uniform distribution model is not quite right, especially for the multiple-channel AlGaN/GaN heterostructures. Besides, it is found the exponential distribution model possibly matches the actual distribution of the surface donor states better, which allows the 2DEG to form in each channel structure during the calculation. The exponential distribution model would be helpful in the research field.

Keywords: AlGaN/GaN, surface states, exponent distribution

PACS: 81.05.Ea, 73.20.At, 73.40.Kp **DOI:** 10.1088/1674-1056/ac0792

1. Introduction

AlGaN/GaN heterostructure devices have been widely used in high-power, high-frequency electronic devices, because of their wide band gap and high electron mobility.[1–5] The unique electrical properties of the AlGaN/GaN heterostructures benefit from the high density and high mobility two-dimensional electron gas (2DEG), which is formed by the spontaneous and piezoelectric polarization charges at the heterointerface.[6] The donor states on the AlGaN/GaN surface have been widely considered as the source of the electrons in the 2DEG.[7–11] Specifically, Smorchkova *et al.*[7] found the 2DEG appeared in $Al_{0.27}Ga_{0.73}N$/GaN heterostructure when the thickness of the AlGaN barrier was more than 3 nm. The critical thickness of the AlGaN barrier, that is, the minimum thickness allowed the existence of 2DEG, was determined by the energy level position of the donor states on the AlGaN surface. Ibbetson *et al.*[8] found the surface donor states were the actual source of the electrons in the 2DEG and the energy level position of the donor states was fixed, which was 1.65 eV below the conduction-band minimum (CB_{min}) on the $Al_{0.34}Ga_{0.66}N$/GaN heterostructure surface. Similarly, the valence band maximum can be expressed as VB_{max}. On the other hand, Koley *et al.*[9] found the position of donor states was not fixed and the bare surface barrier height (BSBH) varied according to the AlGaN barrier thickness and the doping concentration. The surface state density can be estimated based on the value of BSBH. Higashiwaki *et al.*[10] found the surface barrier height monotonically increased with the AlGaN barrier thickness and the surface donor states distributed over a range of energies. Gordon *et al.*[11] found the highest occupied surface states were about 1 eV below the CB_{min} on surfaces. These models, which consider the electrons in the 2DEG coming from the surface donor states, have been widely used in the analysis of GaN based multiple-channel devices.[12–14] However, the precise features of donor states distribution on AlGaN/GaN surfaces are still unclear. In previous reports, the density of surface donor states is constant over the range of energy levels.[9,11]

In this work, a common AlGaN/GaN heterostructure and a triple-channel AlGaN/GaN heterostructure are used for Schottky barrier diodes (SBDs), which can provide the carrier concentration profiles of the two materials by *C*–*V* profiling technique.[15] On the other hand, the carrier concentration profiles can be confirmed by calculation through material structures.[11,16–18] The features of surface donor states distribution are directly related to the carrier concentration profiles in calculation. In our experiments, it is found that the uniform distribution model of surface donor states is not right and the exponential distribution model possibly matches the actual distribution better, especially for the multiple-channel

*Project supported by the Science & Technology Plan of Guangdong Province, China (Grant Nos. 2019B010132001 and 2019B010132003), the joint funding of the Nature Science Foundation of China (NSFC) & the Macao Science and Technology Development Fund (FDCT) of China (Grant No. 62061160368), the National Key Research and Development Program of China (Grant Nos. 2016YFB0400105 and 2017YFB0403001), and the Zhuhai Key Technology Laboratory of Wide Bandgap Semiconductor Power Electronics, Sun Yat-sen University, China (Grant No. 20167612042080001).

†Corresponding author. E-mail: zhbaij@mail.sysu.edu.cn

© 2021 Chinese Physical Society and IOP Publishing Ltd

AlGaN/GaN heterostructures.

2. Experiment and analysis

The epitaxy structures of the common AlGaN/GaN heterostructure and the triple-channel AlGaN/GaN heterostructure are illustrated in Fig. 1(a), and the optical microscope photograph of the SBDs are shown in Fig. 1(b).

Samples are grown by metal-organic chemical vapor deposition (MOCVD) system on *c*-plane sapphire substrates. In epitaxial growth, the common AlGaN/GaN heterostructure starts with an about 20-nm AlN nucleation layer followed by 3-μm unintentionally doped (UID) GaN buffer layer. The channel structure is on the UID GaN buffer layer, consisted of 200-nm UID GaN channel layer, 1-nm UID AlN spacer and 10-nm UID $Al_{0.27}Ga_{0.73}N$ barrier layer from the bottom up. The epitaxy structure of the common AlGaN/GaN heterostructure has been shown in the left half of Fig. 1(a). The triple-channel AlGaN/GaN heterostructure is obtained by inserting two additional channel structures into the common AlGaN/GaN heterostructure. Each of the additional channel structures consists of 10-nm UID GaN channel layer, 1-nm UID AlN spacer, 1-nm UID AlGaN layer, 8-nm Si-doped $Al_{0.27}Ga_{0.73}N$ layer whose doping concentration is 2×10^{18} cm^{-3} and 1-nm UID $Al_{0.27}Ga_{0.73}N$ layer from the bottom up. The two additional channel structures are shown in the right half of Fig. 1(a). The insertion position is 10 nm below the AlN spacer/GaN buffer interface of the common AlGaN/GaN heterostructure.

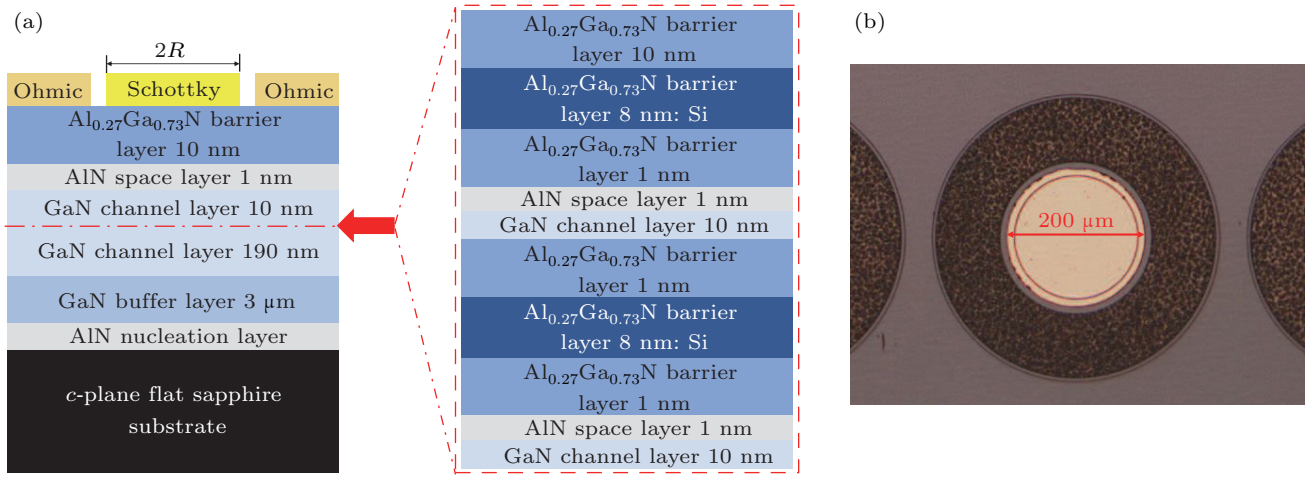


Fig. 1. (a) The epitaxy structures of the common AlGaN/GaN heterostructure and the triple-channel AlGaN/GaN heterostructure. (b) The optical microscope photograph of the SBDs and the diameter of the Schottky contact is 200 μm.

The two SBDs are fabricated as the same as the following process. The mesas are fabricated by inductively coupled plasma reactive ion etching (ICP-RIE), and the etching depth of mesas are 200 nm. Then, ohmic contacts consisting of Ti/Al/Ni/Au (20/80/20/60 nm) are formed by rapid thermal annealing (RTA) at 850 °C for 30 s in nitrogen condition. In the final step, the Schottky contacts are formed by depositing Ni/Au (20/60 nm). The radius of the Schottky contacts is 100 μm, which has been shown in Fig. 1(b).

The capacitance–voltage (*C*–*V*) curves of the two SBDs are measured at room temperature and the frequency of the alternating voltage (AC) signal is 100 kHz. The carrier concentration profiles can be acquired by calculation as follows:[15]

$$D=\frac{\varepsilon_0\varepsilon_s S}{C}, \tag{1}$$

$$N(D)=\frac{2\mathrm{d}V}{q\varepsilon_0\varepsilon_s S^2\,\mathrm{d}\,(1/C^2)}, \tag{2}$$

where D is the depletion depth, $N(D)$ is the carrier concentration, S is the Schottky contact area, ε is the vacuum dielectric constant, ε_s is the relative dielectric constant, and q is the electron charge.

The *C*–*V* curves of the common AlGaN/GaN heterostructure and the triple-channel AlGaN/GaN heterostructure are shown in Fig. 2(a). The carrier concentration profiles over depths of the common and triple-channel AlGaN/GaN heterostructures are shown in Fig. 2(b). The peak value of the carrier concentration in the common AlGaN/GaN heterostructure is 5.65×10^{19} cm^{-3}. There are three peaks of the carrier concentration in the triple-channel AlGaN/GaN heterostructure, the peak values are 5.86×10^{19} cm^{-3}, 1.34×10^{18} cm^{-3} and 4.21×10^{19} cm^{-3} from the surface down, respectively. It means there are three 2DEGs in the triple-channel AlGaN/GaN heterostructure.

On the other hand, the distribution of carrier concentration can be confirmed by calculation through material structures. The AlGaN/GaN heterostructures possess polarized wurtzite structures, having dipoles in the [0001] direction. In the absence of external fields, the total polarization consists of spontaneous and piezoelectric polarization, which can be calculated as follows:[16,17]

$$P_{\mathrm{total}}=2\frac{a'-a}{a}(1-c_{\mathrm{relax}})\left(e_{31}-e_{33}\frac{c_{13}}{c_{33}}\right)$$

$$\times\left(1-\frac{e_{33}^2}{C_{33}}\frac{1}{\left(\varepsilon+\frac{e_{33}^2}{C_{33}}\right)}\right)$$
$$+\frac{e_{33}^2}{C_{33}}\frac{1}{\left(\varepsilon+\frac{e_{33}^2}{C_{33}}\right)}\left(n_{s2D}+\Delta P_{SP}\right), \quad (3)$$

where a and a' are the lattice constants of the the upper and lower parts of the heterostructures respectively. c_{relax} is the relaxation coefficient. e_{31} and e_{33} are the piezoelectric coefficients, and C_{13} and C_{33} are the elastic constants. n_{s2D} is the concentration of 2DEG. ΔP_{SP} equals to the spontaneous polarization of the lower part of the heterostructure minus the spontaneous polarization of the upper part of the heterostructure. ε is the permittivity of the materials.

The charge distribution ρ can be calculated by the self-consistent Poisson equation as follows:[18]

$$\nabla\cdot\left(\begin{bmatrix}\varepsilon_{11}&0&0\\0&\varepsilon_{11}&0\\0&0&\varepsilon_{33}+\frac{e_{33}^2}{C_{33}}\end{bmatrix}\nabla\varphi\right)=-\rho+\nabla\cdot\begin{bmatrix}0\\0\\P_{total}\end{bmatrix}, \quad (4)$$

where ε_{ij} is the second-ranked permittivity tensor, e_{33} is a piezoelectric coefficient, C_{33} is an elastic constant, φ is the electrostatic potential, and P_{total} is the total polarization.

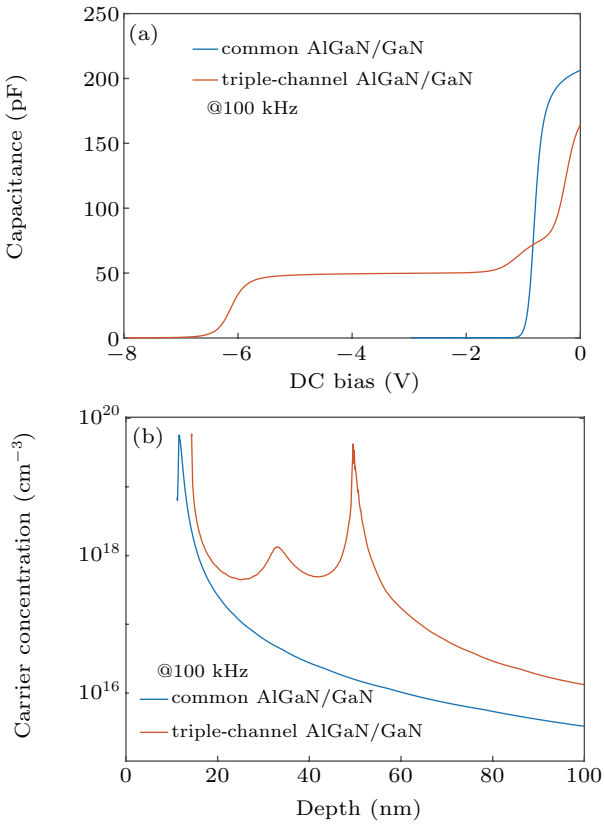


Fig. 2. (a) The *C*–*V* curves of the common AlGaN/GaN heterostructure and the triple-channel AlGaN/GaN heterostructure. (b) The carrier concentration profiles over depths of the two AlGaN/GaN heterostructures.

Equations (3) and (4) are used to calculate the carrier concentration distribution of the common AlGaN/GaN heterostructure with a uniform distribution model of the surface donor states. In our models, the highest surface donor states are 1 eV below the CB_{min} on surface based on the previous literature, it means the critical surface barrier height is 1 eV.[11] So, the uniform distribution model of the surface donor states of the common AlGaN/GaN heterostructure can be expressed as follows:[11]

$$n_{surface}=n_0\left(VB_{max}<E<CB_{min}-\Phi_c\right), \quad (5)$$

where E is the forbidden bandwidth. Φ_c is the critical surface barrier height, and its value is 1 eV. n is the constant density of the surface donor states, whose unit is cm^{-2}·eV^{-1}. CB_{min} is the conduction-band minimum on surface.

The calculation results indicate the calculated peak value of the carrier concentration is 5.65×10^{19} cm^{-3} in the common AlGaN/GaN heterostructure when the n is 2.23×10^{13} cm^{-2}·eV^{-1}. The band structure and the distribution of carrier concentration of the common and triple-channel AlGaN/GaN heterostructures are shown in Fig. 3.

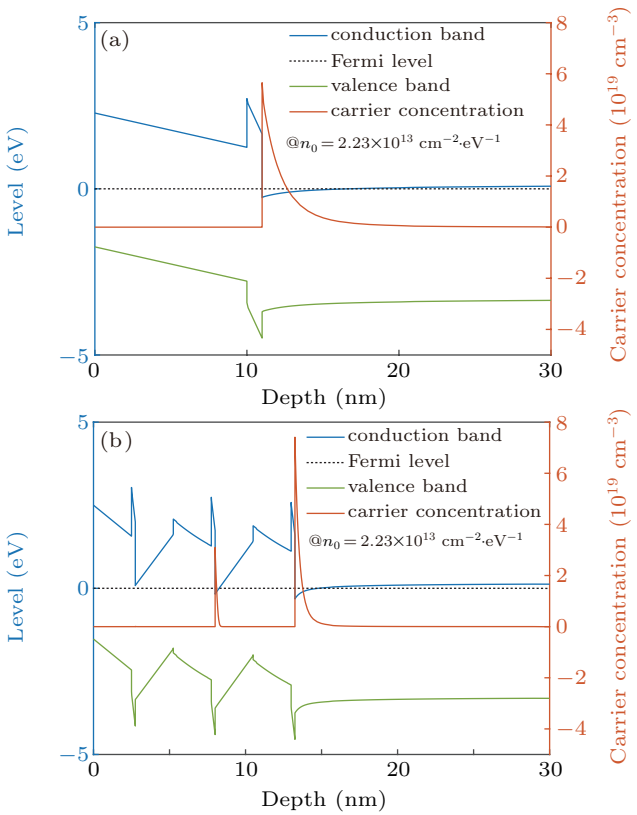


Fig. 3. The band structure and the distribution of carrier concentration in the common AlGaN/GaN heterostructure (a) and the triple-channel AlGaN/GaN heterostructure (b) with $n=2.23\times10^{13}$ cm^{-2}·eV^{-1}.

As shown in Fig. 3(b), in the uniform distribution model, there are only two 2DEGs in the triple-channel AlGaN/GaN heterostructure when n is 2.23×10^{13} cm^{-2}·eV^{-1}. The results show that the surface donor states of the triple-channel AlGaN/GaN heterostructure do not obey the uniform distribution because it cannot provide enough electrons to form three separate 2DEGs.

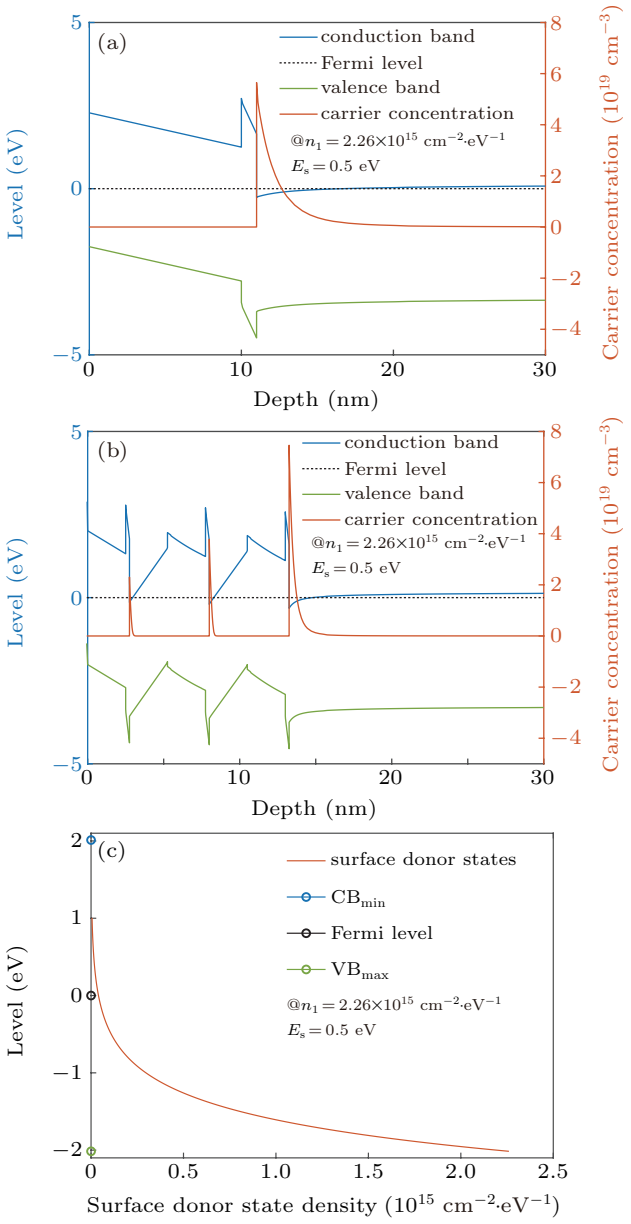


Fig. 4. The band structure and the distribution of carrier concentration in the common AlGaN/GaN heterostructure (a) and the triple-channel AlGaN/GaN heterostructure (b) with $n_1 = 2.26 \times 10^{15}$ cm^{-2}·eV^{-1} and $E_s = 0.5$ eV. (c) The distribution of the surface donor states. The blue, black and green circles resperent the CB$_{min}$, Fermi level and VB$_{max}$ on surface, respectively.

According to the previous experimental and calculating results, we guess that the level of the surface donor states is closer to the valence band on surface, and the density of the surface donor states is higher. Hence, the exponential distribution model possibly matches the actual distribution of the surface donor states better. The exponential distribution model of the surface donor states in AlGaN/GaN heterostructures can be expressed as follows:

$$n_{\text{surface}} = n_1 \exp\left(-\frac{E-\text{VB}_{\max}}{E_s}\right), \quad (\text{VB}_{\max} < E < \text{CB}_{\min} - \Phi_c), \tag{6}$$

where n_1 is the maximum of the surface donor state density in exponential distribution model, whose unit is cm^{-2}·eV^{-1}. CB$_{min}$ is the conduction-band minimum on surface. The range of the exponential distribution is determined by E_s. When $E_s = 0.5$, the highest occupied surface states are 1 eV below the CB$_{min}$ on surfaces according to Eq. (6). The distribution has been shown in Fig. 4(c).

In this model, calculations show that the peak value of the carrier concentration is 5.65×10^{19} cm^{-3} in the common AlGaN/GaN heterostructure when n_1 equals to 2.26×10^{15} cm^{-2}·eV^{-1}. The band structure and the distribution of carrier concentration of the common and triple-channel AlGaN/GaN heterostructures have been shown in Figs. 4(a) and 4(b). The distribution of the surface donor states is shown in Fig. 4(c). The location of 0 eV in Fig. 4(c) means the valence-band maximum on surface.

As shown in Fig. 4(b), there are three separate 2DEGs in the triple-channel AlGaN/GaN heterostructure when $n_1 = 2.26 \times 10^{15}$ cm^{-2}·eV^{-1} and $E_s = 0.5$ eV. The calculation results show the exponential distribution model possibly matches the actual distribution of the surface donor states better, because it allows the 2DEG to form in each channel structure of the triple-channel AlGaN/GaN heterostructure during calculation. The peak values of the carrier concentration are different from the actual peak values, which indicates that the exponential distribution model is still not the actual distribution model of the surface donor states. But the exponential distribution model matches the actual distribution better compared with the uniform distribution model.

3. Conclusion

In this work, we try to verify the uniform distribution model of the surface donor states in AlGaN/GaN heterostructures by experiments and calculations, which has been widely used in the theoretical calculation. A common AlGaN/GaN heterostructure and a triple-channel AlGaN/GaN heterostructure SBDs have been fabricated to verify the models about the distribution of surface donor states. The carrier concentration profiles of the two SBDs are obtained by *C*–*V* profiling technique. On the other hand, the carrier concentration profiles can be confirmed by calculation through the epitaxy structures of the AlGaN/GaN heterostructures. The features of surface donor states distribution are directly related to the carrier concentration profiles in calculation, so the models about the distribution of surface donor states can be verified by calculating. In the calculation, the highest occupied surface states are 1 eV below the CB$_{min}$ on surfaces. The results show the uniform distribution model is not right, because the surface donor states in this model cannot provide enough electrons to form three separate 2DEGs in the triple-channel AlGaN/GaN heterostructure. Compared to the uniform distribution model, the exponential distribution model possibly matches the actual distribution of the surface donor states better, because it allows the

2DEG to form in each channel structure of the triple-channel AlGaN/GaN heterostructure during calculation. Although the exponential distribution model is still different from the actual distribution model of the surface donor states, we think it would be helpful in the research field.

Acknowledgement

The authors are grateful to Professor Xin-Qiang Wang at Peking University for the support of the common AlGaN/GaN heterostructure and the triple-channel AlGaN/GaN heterostructure samples.

References

[1] Vurgaftman I, Meyer J R and Ram-Mohan L R 2001 *J. Appl. Phys.* **89** 5815

[2] Rajan S, Waltereit P, Poblenz C, Heikman S J, Green D S, Speck J S and Mishra U K 2004 *IEEE Electron. Device Lett.* **25** 247

[3] Veksler D, Aniel F, Rumyantsev S, Shur M S and Gaska R 2006 *Proceedings of the 5th IEEE Conference on Sensors*, October 22–25, 2006, Daegu, Korea (South), p. 323

[4] Jin C, Pavlidis D and Considine L 2013 *IEICE Trans. Electron.* **95** 1348

[5] Shinohara K, Regan D C, Tang Y and Corrion A L 2013 *IEEE Trans. Electron. Devices* **60** 2982

[6] Ambacher O, Smart J, Shealy J R, Weimann N G, Chu K, Murphy M, Schaff W J, Eastman L F, Dimitrov R, Wittmer L, Stutzmann M, Rieger W and Hilsenbeck J 1999 *J. Appl. Phys.* **85** 3222

[7] Smorchkova I P, Elsass C R, Ibbetson J P, Vetury R, Heying B, Fini P, Haus E, Denbaars S P, Speck J S and Mishra U K 1999 *J. Appl. Phys.* **86** 4520

[8] Ibbetson J P, Fini P T, Ness K D, Denbaars S P, Speck J S and Mishra U K 2000 *Appl. Phys. Lett.* **77** 250

[9] Koley G and Spencer M G. 2001 *J. Appl. Phys.* **90** 337

[10] Higashiwaki M, Chowdhury S, Miao M, Swenson B L, Van de Walle C G and Mishra U K 2010 *J. Appl. Phys.* **108** 63719

[11] Gordon L, Miao M S, Chowdhury S, Higashiwaki M, Mishra U K and Walle C G V D 2010 *J. Phys. D-Appl. Phys.* **43** 505501

[12] Wang Y, Yang L, Wang Z, Ao J and Hao Y 2016 *Phys. Status Solidi A* **213** 1252

[13] Yu C, Lin C and Wu Y 2020 *IEEE T. Nanotechnol.* **19** 439

[14] Erine C, Ma J, Santoruvo G and Matioli E 2020 *IEEE Electron. Device Lett.* **41** 321

[15] Kroemer H, Chien W Y, Harris J S and Edwall D D 1980 *Appl. Phys. Lett.* **36** 295

[16] Ashok A, Vasileska D, Goodnick S M and Hartin O L 2009 *IEEE Trans. Electron. Devices* **56** 998

[17] Anwar A F M, Webster R T and Smith K V 2006 *Appl. Phys. Lett.* **88** 203510

[18] Jogai B, Albrecht J D and Pan E 2003 *J. Appl. Phys.* **94** 3984